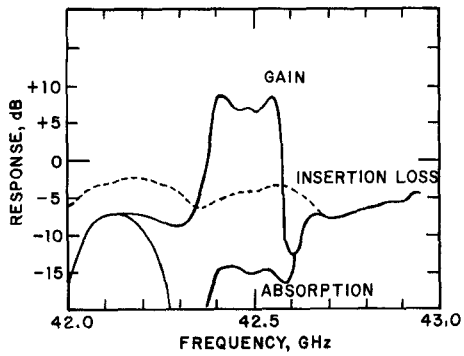

Fig. 2. Single-stage maser bandpass.

of 42.5 GHz. The observed inversion ratio was 1.2 with a pump power of 55 mW at the dewar input. The pump has a center frequency of 86.75 GHz and was distributed over 420 MHz peak to peak at a 20-kHz modulation rate. The sensitivity of gain to pump power level indicated that an increase of 4 dB in pump power was required in order to saturate the pump transitions (i.e., 0.25-dB gain change for 1-dB pump power change at saturation). When pump waveguide losses are accounted for, the pump power needed is about 6 times higher than that required for comparable performance with the 24-GHz maser. Thus, pump power on the order of 2.5 W would be required for a four-stage reflected wave maser to yield a bandwidth of 1 GHz and net gain of 30 dB at center frequencies near 40 GHz. A more modest pump power of 500 mW would yield a bandwidth of 200 MHz.

When the single-stage maser was placed ahead of a room temperature mixer receiver, a single sideband receiver noise temperature (including the contribution from a standard gain horn on the maser input) of 515 K was measured. The follow-up receiver contribution was measured as 480 K. The difference of these two measurements is the combined maser and horn noise temperature. These noise temperatures were measured at a center frequency of 42.5 GHz using ambient and liquid nitrogen temperature absorber as reference loads at the aperture of the standard gain horn. When the estimated noise contributions of the horn and input waveguide (from 300 to 4.6-K cryogenic temperature) were accounted for, the maser noise temperature at the cooled circulator input was estimated to be 14 K. The theoretical noise temperature at this point is 6.6 K, assuming 0.5-dB loss per pass in the circulator and 2.3-dB loss in the maser structure. Considering the uncertainty in the estimated maser noise temperature, any agreement between experimental and theoretical estimates is fortuitous.

IV. Conclusion

We have shown that pink ruby is useful as a maser material for frequencies in excess of 43 GHz. Pump power requirements set a limit to the bandwidth which is practical, but bandwidths exceeding 1 GHz are possible if sufficient pump power and FM deviation are available. The system temperature-bandwidth ratio should be superior to those of other devices presently operating in this frequency range.

Acknowledgment

This paper presents work which was made possible through prior maser research carried out at the Jet Propulsion Laboratory, California Institute of Technology, under a Contract with the National Aeronautics and Space Administration. The inversion ratio measurements described here were a cooperative effort between the National Radio Astronomy Observatory and JPL, under a contract from NRAO.

References

[1] Ruby material supplied by Union Carbide Corp., Crystal Products Div., 60 degree, CZ Boule, SIQ grade.
[2] E. Makhov *et al.*, *Phys. Rev.*, vol 109, p 1399, 1958.
[3] C. R. Moore and R. C. Clauss, *IEEE Trans. Microwave Theory Tech.*, vol. MTT-27, p. 249, 1979.
[4] W. H. Higa and E. Wiebe, *Cryog. Technol.*, vol. 3, pp. 47 & 50, 1967.
[5] W. H. Higa and E. Wiebe, "One million hours at 4.5 Kelvin," presented at the Cryocooler Applications Conf., sponsored by the National Bureau of Standards, Boulder, CO, Oct. 1977.
[6] R. Berwin, R. Clauss, and E. Wiebe, in *Space Programs Summary 37-56, vol. II*, Jet Propulsion Lab, Pasadena, CA, Mar. 1969.
[7] R. Clauss, in *SPS 37-61, vol. III*, Jet Propulsion Lab, Pasadena, CA, 1970, p 90.
[8] A. E. Siegman, *Microwave Solid-State Masers*. New York: McGraw-Hill, 1964.
[9] C. R. Moore, "A *K*-band ruby maser with 500-MHz bandwidth," *IEEE Trans. Microwave Theory Tech.*, vol. MTT-28, p. 149, 1980.
[10] P P. Cioffi, "Approach to the ideal magnetic circuit concept through superconductivity," *J. Appl. Phys.*, vol. 33, pp. 875-879, Mar. 1962.

Automatic Permittivity Measurements in a Wide Frequency Range: Application to Anisotropic Fluids

J. P. PARNEIX, C. LEGRAND, AND S. TOUTAIN

Abstract—**In this paper a new dielectric measurements method in the range 200 MHz-18 GHz is reported. The main features of the system are the following: a) automatic determination of the sample complex permittivities for each step of frequency previously chosen by using a numerical process; b) cells requiring only a very small sample volume (typically lower than .1 cm^3); and c) cell structure allowing the dielectric characterization of anisotropic substances.**

I. Measurement Method Description

By using classical methods, the determination of the complex permittivity ($\epsilon^* = \epsilon' - j\epsilon''$) of dielectric materials is generally carried out for singular frequencies which can be very scarce in the microwave region typically one or two points for a decade range [1]. Furthermore, these methods are difficult to work out, and they often use a very large sample volume. The original method which is presented in this paper attempts to remove all these difficulties.

A. Basic Operation

Fig. 1 shows a simplified diagram of the measurement system. The basic device is a H.P. 8410 network analyzer connected to a H.P. 9825 computer. The sweep oscillator is phase locked by a Dana E.I.P 381 microwave counter. System calibration and operation is as follows.

a) The network analyzer is calibrated by using successively a calibrating short, an open circuit, and a sliding load.

Manuscript received February 22, 1982; revised June 9, 1982.
The authors are with the Centre Hyperfrequences et Semiconducteurs, Laboratoire Associe au C.N.R.S. n 287, Universite de Lille I-Bat. P3, 59655 Villeneuve D'Ascq Cedex, France.

0018-9480/82/1100-2015$00.75 ©1982 IEEE

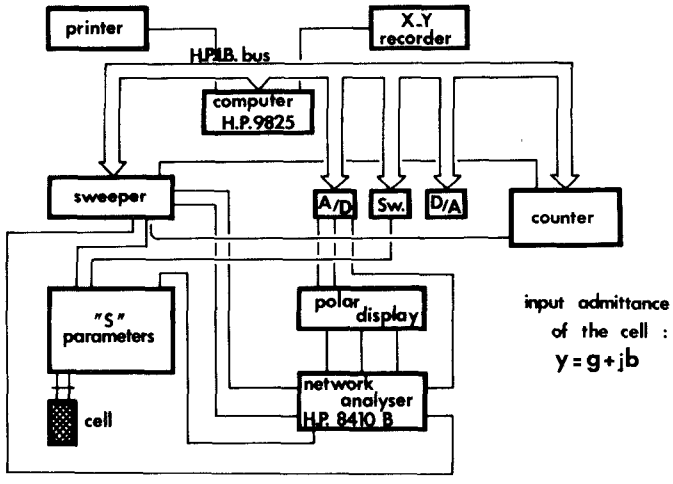

Fig 1 The experimental setup.

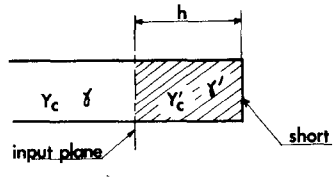

Fig. 2. The simplified diagram of the system.

b) The cell is connected to the analyzer output. The analyzer gives automatically the normalized conductance g and susceptance b in the input plane of the cell. The results are stored in the computer memory unit.
c) The data are introduced in to a numerical process which gives directly the permittivity of the sample filling in the cell.

B. Numerical Determination of Permittivities: Coaxial Structures

Fig. 2 schematically shows the simplified system to be solved. It consists of a h-length coaxial line, filled in with the unknown dielectric substance whose complex permittivity is $\epsilon_0\epsilon_f^*$. This coaxial line is short circuited at one end and a thin sheet of mica defined the input air dielectric interface.

By using well-known transmission-line theories [1], it can be shown that the Y_e' input admittance of the line (characteristic admittance Y_c'), can be written as

$$Y_e' = Y_c' \coth(\gamma' h) \tag{1}$$

where the propagation factor γ' is given by

$$\gamma' = \alpha' + j\beta' = j\omega(\epsilon_0\epsilon_f^*)^{1/2} \tag{2}$$

The network analyzer gives the reduced admittance y_e' according to the Y_c characteristic admittance of the air coaxial line. Then (1) yields

$$y_e' = \frac{Y_c'}{Y_c}\coth(\gamma' h). \tag{3}$$

The characteristic admittance ratio is defined as

$$\frac{Y_c'}{Y_c} = \frac{\gamma'}{\gamma}. \tag{4}$$

γ is the air propagation factor in the main line given by

$$\gamma = j\beta = j\omega(\epsilon_0)^{1/2} = j2\Pi\frac{f}{c} \tag{5}$$

where f and c are the frequency and the light velocity, respectively.

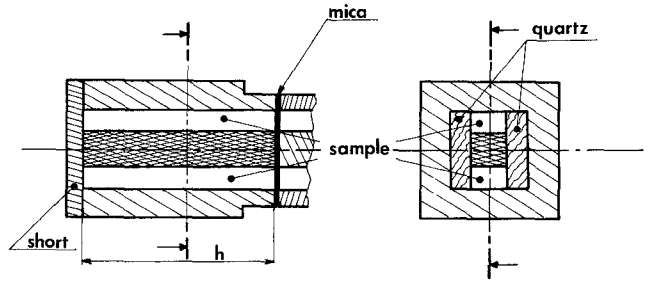

Fig. 3 The measurement cell.

Equation (3) then becomes

$$y_e' = g + jb = \frac{\alpha' + j\beta'}{j\beta}\coth(\gamma' h) \tag{6}$$

which may be rearranged to

$$x + jy = -j(u + jv)\cdot\coth(u + jv) \tag{7}$$

with

$$\begin{cases} x = g\beta h \\ y = -b\beta h \end{cases} \quad \text{and} \quad \begin{cases} u = A\beta h = \alpha' h \\ v = B\beta h = \beta' h \end{cases}.$$

Finally, the real and imaginary parts of (4) furnish the relations

$$\begin{cases} x = \dfrac{vsh2u - u\sin 2v}{ch2u - \cos 2v} \\ y = \dfrac{ush2u + v\sin 2v}{ch2u - \cos 2v} \end{cases}. \tag{8}$$

By using (2), (5), and (7), the real and imaginary parts of ϵ_f^* then follow:

$$\epsilon_f^* = \epsilon_f' - j\epsilon_f''$$
$$\begin{cases} \epsilon_f' = B^2 - A^2 \\ \epsilon_f'' = 2AB \end{cases}. \tag{9}$$

For a given couple of x, y values, the numerical solution of system (8) is achieved, then ϵ_f' and ϵ_f'' are deduced. One difficulty remains concerning this calculation. Indeed, the transcendental equations (8) show an infinity of solutions. This difficulty is removed assuming first a lossless material ($x = 0$) and calculating the approximate ϵ_f' values. Then, the only realistic value is kept (for instance, in comparison with lower frequency data), and is used to solve the overall system (8).

II. Cell Description

The main features of the experimental cell are the following:

a) a small sample volume on account of the small quantities available; b) a wave propagation mode allowing the characterization of uniaxial anisotropic substances. The electric-field lines must be parallel to each other. Thus, there are two measurement configurations: either the electric-field direction is parallel to the optical axis ($\epsilon_{\parallel}^*$) or perpendicular to it ($\epsilon_{\perp}^*$); and c) optimization of geometrical sizes to allow a wide frequency range of utilization.

A simplified diagram of the cell is given in Fig. 3. It consists in a short-circuited rectangular hybrid structure with the same geometrical sizes as the standard coaxial APC7 connector. The input plane is a sheet of mica. The gap between the internal and external conductors is partially filled in with quartz which enables us, first, to get an homogeneous electric field inside the sample and, secondly, to limit the volume of sample. We chose this material because of its very low thermal coefficient and low dielectric losses. Moreover, it is easy to machine with accuracy.

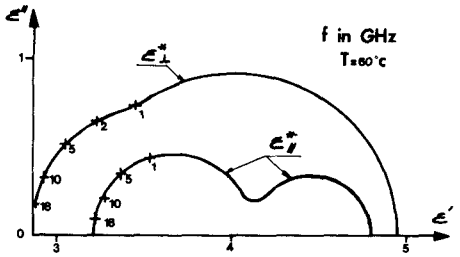

Fig. 4. Cole Cole plots of p-methoxyphenylazoxy-p'-butylbenzene in the nematic phase. $\epsilon_{\parallel}^*$: electric field $\parallel$ optical axis. $\epsilon_{\perp}^*$: electric field $\perp$ optical axis.

III. Calculation Procedure of the Sample Permittivity

Two stages are necessary in the calculation. First, a fictitious permittivity ϵ_f^* is calculated in the same way as before, assuming the cell to be coaxial of the same length and filled homogeneously with the sample. Then, the substance permittivity ϵ^* is deduced using a linear relationship

$$\epsilon_f^* = (1-\theta)\epsilon_q + \epsilon^*\theta$$
$$\epsilon^* = \epsilon' - j\epsilon'' \tag{10}$$

where ϵ_q is the quartz permittivity which is supposed to be real and θ is a filling factor. Then

$$\begin{cases} \epsilon' = \dfrac{\epsilon_f' - (1-\theta)\epsilon_q}{\theta} \\ \epsilon'' = \dfrac{\epsilon_f''}{\theta} \end{cases} \tag{11}$$

The filling factor θ can be calculated in the following way: in spite of the hybrid character of the cell, a quasi-TEM propagation-mode approximation can be assumed. Then, using a numerical method (finite difference method), it is easy to calculate ϵ_f' as a function of ϵ' by solving Laplace's equation in a cross-section plane of the cell [2].

We verified the linear relationship between ϵ_f' and ϵ'. The slope of the straight line gives θ.

The validity of all approximations is tested using standard liquids. Particularly, we have verified that no spurious higher order mode is propagating in the structure up to 18 GHz. In this bandwidth, the quasi-TEM approximation gave consistent results for low-loss dielectric materials with ϵ' values up to 7. In actual fact, the measurement accuracy is similar to the accuracy of usual measurement methods, namely the overall uncertainty is lower than 2 percent for ϵ' and 5 percent for ϵ''. Moreover, this method allows the direct plotting of spectra in the whole bandwidth.

IV. Applications

The process has been applied to the dielectric characterization of nematic liquid crystals in the microwave range. These substances are uniaxial, and the orientation of the sample optical axis with respect to the electric-field direction is achieved by using a magnetic field [3]. For example, we give in Fig. 4 the results obtained for a nematic compound in each direction of measurement: the parallel direction ($\epsilon_{\parallel}^*$), the perpendicular direction ($\epsilon_{\perp}^*$). The full line concerns the data we obtained by using conventional techniques [4]. The crosses are relative to the automatic process described before (only a few points are given). As we can see, the agreement is quite satisfying.

Such a process can be applied to other mesomorphic substances such as smectics, but also to liquids and isotropic or anisotropic solids. Obviously, in the last case, the sample optical axis has to be defined with respect to the electric field.

References

[1] N. E. Hill, W E. Vaughan, A. H. Price, and M. Davies, *Dielectric Properties and Molecular Behaviour*. London: Van Nostrand, 1969.
[2] H. E. Green, *IEEE Trans. Microwave Theory Tech.*, vol. MTT-13, p. 676, 1965.
[3] For a general review of the physical properties of liquid crystals see, for example: P. G. De Gennes, *The Physics of Liquid Crystal*. Oxford: Clarendon Press, 1974.
[4] J. P. Parneix, A. Chapoton, E. Constant, *J. Phys*, vol. 36, p. 1143, 1975.

Broad-band GaAs Monolithic Amplifier Using Negative Feedback

PHILIP A. TERZIAN, DOUGLAS B. CLARK AND RAYMOND W. WAUGH

Abstract—**A monolithic amplifier covering the 1–7-GHz frequency band has been fabricated using negative feedback. Small signal power gain of 6.0 dB ± 0.2 dB was achieved with maximum input and output VSWR of 2.3:1 and 1.7:1, respectively. Design considerations and processing techniques for active and passive elements are presented along with detailed performance data.**

I. Introduction

The use of distributed reactive matching elements and quadrature couplers in a balanced circuit are common in hybrid broad-band microwave amplifier designs. This technique has the advantages of simultaneous low reflection coefficients and maximum gain over bands up to several octaves. The higher dielectric constant of GaAs as compared to alumina results in only a 30 percent size reduction of distributed passive elements. For monolithic integrated circuits, where it is desirable to minimize the space used for passive elements, the use of lumped elements is an attractive alternative.

Negative feedback hybrid FET amplifiers are gaining popularity for broad-band application below 12 GHz. Several authors have presented data and design guidelines for selecting feedback elements to minimize input and output reflection coefficients consistent with maximum flat gain and minimum noise figure [1], [2]. Since these feedback designs employ lumped elements, this type of circuit is an obvious choice for monolithic applications.

The design of this monolithic amplifier utilizes experience gained in the development of various hybrid feedback designs nearing production. These hybrid circuits were used to obtain an insight into the FET geometry and circuit topology required to achieve desired amplifier performance.

II. Amplifier Design

The selection of a FET with sufficient transconductance is essential for the successful application of feedback techniques. Computer aided design and experience have shown that a 1000-μm gate width device with a transconductance of at least 80

Manuscript received May 17, 1982; revised July 7, 1982.
The authors are with the Narda Microwave Corporation, 214 Devcon Drive, San Jose, CA 95112.

0018-9480/82/1100-2017$00.75 ©1982 IEEE